

X-ray emission from middle-aged pulsars

Rosalba Perna^{1,3}, Jeremy Heyl^{2,3} & Lars Hernquist³

ABSTRACT

We present a simple, unified model which accounts for properties of the X-ray emission from the three middle-aged pulsars PSR 1055-52, PSR 0656+14 and PSR 0630+18 (Geminga). The X-ray radiation from these objects is pulsed more strongly at energies above a transition point around 0.5 keV. In addition, the phase of the pulses shifts by about $80^\circ - 100^\circ$ degrees around the same point. Geminga also has the peculiarity that its pulsed fraction *decreases* in the 0.3-0.5 keV energy range, attaining a minimum near 0.5 keV. We show that a two-component hydrogen atmosphere is able to account for these disparate features. In our model, the hotter component is powered by particle bombardment and is restricted to the polar regions, while the cooler one covers the entire stellar surface. The two components also differ in their emission patterns, with the hard and soft contributions coming from areas radiating into fan and pencil beams, respectively.

Subject headings: pulsars: general — stars: neutron — X-rays: stars

1. Introduction

X-ray emission from cooling neutron stars (NSs) had been predicted and studied in detail already in the early 1960's (Chiu & Salpeter 1964; Tsuruta 1964). However, it was not until the late 70's that the *Einstein* Observatory first detected radiation from isolated NSs, and until the *ROSAT* era (the 1990's) that more detailed information on the spectral characteristics and pulsed fraction (Pf) could be obtained.

Thermal radiation due to cooling can be best observed in a small subset of pulsars which are middle-aged and have characteristic lifetimes $\tau \sim 10^5$ yr. In younger pulsars, such as the Crab, X-rays of magnetospheric origin often dominate over thermal emission, while older ones are too cold to have any observable radiation due to cooling. So far, the three best candidates for which thermal emission has likely been detected are PSR 1055-52, PSR 0656+14 and PSR 0630+18.

¹Harvard Junior Fellow

²*Chandra* Fellow

³Harvard-Smithsonian Center for Astrophysics, 60 Garden Street, Cambridge, MA 02138

Apart from a non-thermal, power-law component dominating the high-energy tail (this is particularly evident in PSR 0656+14; Greiveldinger et al. 1996) and which is thought to be due to magnetospheric processes, the bulk of the emission between $\sim 0.1 - 1$ keV is well fitted by a double blackbody at two different temperatures. The ratio of the area of the hotter component to the colder one is typically very small (\sim a few $\times 10^{-5}$ to a few $\times 10^{-3}$). The colder component has been interpreted as being due to thermal cooling, while the hotter one most likely arises from heated polar caps, with the extra heating being due to bombardment by high-energy particles (Greiveldinger et al. 1996).

An important property of the radiation from all three pulsars (for a review see Becker & Trumper 1997) is a phase shift of $\sim 80^\circ - 100^\circ$ at a transition point which is around 0.5-0.6 keV. The pulsed fraction also shows transitions in its behavior in this region for both PSR 1055-52 and PSR 0656+14. Below ~ 0.5 keV, it is roughly constant at the 10% level, while it rapidly increases after that point to about 20-30% for PSR 0656+14 and to about 80-90% for PSR 1055-52. On the other hand, the pulsed fraction from Geminga shows an intriguing feature: in the PSPC channels 8-28 (i.e. roughly at energies below 0.3 keV) the Pf is much larger than in channels 28-53 (roughly corresponding to the energy range 0.3-0.5 keV): 33% versus 20%. However, as discussed by Page (1995) and Page & Sarmiento (1996), no matter what the surface temperature distribution is, as long as it is not uniform, blackbody emission always gives an increase of the Pf with energy. Detailed modeling by Shibano et al. (1995) shows that realistic atmospheres are able to produce a slight decrease of the Pf with increasing energy, but it is still much smaller than what is observed. A model which could account for the large observed decrease has been presented by Page, Shibano & Zavlin (1995). They assume the presence of warm, magnetized plates on the surface of Geminga, surrounded by cold, unmagnetized regions, with the warmer plates emitting a softer spectrum than the surrounding areas. In this model, Geminga would therefore have different characteristics than the two other objects in the same class.

In this *Letter*, we present a simple model for the emission in the 0.1 \sim 1 keV range that is able to account for the properties of all three pulsars within a unified framework. We model the cooling component as a blackbody modified by a light-element atmosphere; as discussed in the literature (Heyl & Hernquist 1998b, Zavlin, Pavlov & Shibano 1996, Pavlov et al. 1994), this radiation, which emerges through an atmosphere heated from below, is most likely emitted in a “pencil” beam (Pavlov et al. 1994, Zavlin, Pavlov & Shibano 1996). The hotter component, due to particle bombardment of the polar caps, is produced in an atmosphere that is hotter on top, i.e. at lower densities. This is due to the fact that the tenuous upper reaches of the neutron-star atmospheres are extremely inefficient emitters; therefore, as the bombarding particles deposit energy in this region, it heats up dramatically to maintain radiative balance. Meanwhile, the denser layers of the atmosphere which have a larger opacity heat up relatively little. The problem of atmospheres heated from above has been discussed in the literature in the context of slow accretion onto neutron stars (Zane, Turolla & Treves 2000) and the X-ray illumination of normal stars in X-ray binaries (*e.g.* Milgrom & Salpeter 1975). It has been shown that the radiation

from an atmosphere illuminated from above may be emitted in a “fan” pattern (*e.g.* Milgrom & Salpeter 1975). In fact, as one moves away from the normal, the effective photosphere of the atmosphere moves to lower densities due to geometrical effects. In a bombarded atmosphere, these lower densities are hotter, so one sees a hotter and brighter spectrum as one approaches grazing incidence.

We show that a combination of pencil beaming from the cooling component and fan beaming from the hotter polar caps is able to account not only for the magnitude of the pulsations in PSR 1055-52 and PSR 0656+14, but also for the phase shift between the soft and the hard components. Moreover, this same model is able to account also for the *decrease* of the pulsed fraction observed in the soft X-ray emission of Geminga, without requiring any special model for the composition of the surface of this object.

The paper is organized as follows: in §2, we describe in detail the X-ray spectral model; specific applications to PSR 1055-52, PSR 0656+14 and Geminga are discussed in §3; our results are summarized and discussed in §4.

2. X-ray spectrum

We model the local emission from the surface of the star, $n(E, T)$, as a blackbody spectrum modified by the presence of an atmosphere, for which we adopt the semianalytical model developed by Heyl & Hernquist (1998c) with a geometric generalization to study the spectral intensity away from the normal. The dependence of our results on the atmospheric composition will be discussed in §3. We assume that the neutron star has a dipolar magnetic field. With this field geometry and a sufficiently strong intensity, the flux transmitted through the envelope can be approximated as $F \propto \cos^2 \psi$, where $\cos^2 \psi = 4 \cos^2 \theta_p / (3 \cos^2 \theta_p + 1)$ is the angle between the radial direction and the magnetic field (Greenstein & Hartke 1983; Heyl & Hernquist 1998a, 2000); here

$$\theta_p = \arccos(\cos \theta \cos \alpha + \sin \theta \sin \alpha \cos \phi) \quad (1)$$

is the angle that the magnetic pole makes with the normal to the star at position (θ, ϕ) , while α is the angle that it makes with the line of sight. If ξ is the angle between the magnetic dipole and the rotation axis, and χ the angle between the observer’s direction and the rotation axis, then the angle α is given by

$$\alpha = \arccos(\cos \chi \cos \xi + \sin \chi \sin \xi \cos \gamma), \quad (2)$$

with γ being the phase angle.

Outside of the heated polar caps, the local temperature on the star due to thermal cooling is given by

$$T_{\text{th}}(\theta, \phi) = T_p \left[\frac{4 \cos^2 \theta_p}{3 \cos^2 \theta_p + 1} (0.75 \cos^2 \theta_p + 0.25)^{0.2} \right], \quad (3)$$

where, following Heyl & Hernquist (1998a), we have assumed a further dependence of the flux on magnetic field strength scaling as $B^{0.4}$. In Equation (3), T_p is the temperature that the pole would have if there were no reheating.

Now, let β be the angular size of the radius of the polar caps, which are centered around the poles. The hot spot region (in the upper hemisphere) is defined by

$$\theta \leq \beta, \quad \text{if } \alpha = 0 \quad (4)$$

and

$$\begin{cases} \alpha - \beta \leq \theta \leq \alpha + \beta \\ \phi \leq \phi_p \text{ or } 2\pi - \phi \leq \phi_p, \end{cases} \quad \text{if } \alpha \neq 0 \text{ and } \beta \leq \alpha \quad (5)$$

where

$$\phi_p = \arccos \left[\frac{\cos \beta - \cos \alpha \cos \theta}{\sin \alpha \sin \theta} \right]. \quad (6)$$

Here, we have chosen a system of coordinates such that the prime meridian passes through the North pole of the star, at the center of the upper polar cap. The hot spot in the lower hemisphere is defined by the condition $\theta \leq \pi - \beta$, if $\alpha = 0$, and by Equation (5) and Equation (6) with the substitutions $\alpha \rightarrow \pi - \alpha$ and $\phi \rightarrow \pi - \phi$, if $\alpha \neq 0$.

Inside the hot spot, we assume the temperature to be constant, $T_{\text{hs}}(\theta, \phi) = \text{const} \equiv T_{\text{hs}}$. As already discussed, we adopt pencil beaming for the thermal component and fan beaming for the radiation produced in the polar caps, and, for simplicity, we parameterize them with the functions

$$\begin{cases} f_{\text{th}}(\delta) \propto \cos^{n_1}(\delta) \\ f_{\text{hs}}(\delta) \propto \sin^{n_2}(\delta) \end{cases}, \quad (7)$$

where δ is the angle that a photon emitted at a colatitude θ on the star makes with the normal to the surface at the moment of emission. The relation between θ and δ (which is a consequence of the general relativistic effects of light deflection) is given by the ray-tracing function (Page 1995)

$$\theta(\delta) = \int_0^{R_s/2R} x \, du \left/ \sqrt{\left(1 - \frac{R_s}{R}\right) \left(\frac{R_s}{2R}\right)^2 - (1 - 2u)u^2 x^2} \right., \quad (8)$$

having defined $x \equiv \sin \delta$. The value of n_1 in the above equation is found to be roughly unity for an unmagnetized light-element atmosphere (Zavlin, Pavlov & Shibanov 1996) and slightly larger for a magnetized light-element atmosphere (Pavlov et al. 1994), while it is about 0.5 for an atmosphere made of heavy elements (Rajagopal, Romani & Miller 1997). In our calculations we restrict ourselves to this range of values. The exponent n_2 , on the other hand, is treated as a fit parameter and is allowed to vary from source to source, as one would expect the extent of fan beaming in the bombarded atmosphere to depend on the spatial and energy distribution of the bombarding particles which are unknown (and likely to vary among different objects).

The calculation of the emitted spectrum fully accounts for the consequences of gravitational bending of light and gravitational redshift. Let us define $e^{-\Lambda_s} = \sqrt{1 - R/R_s}$, where R is the radius

of the neutron star, and $R_s = 2GM/c^2$ is its Schwarzschild radius. A range of radii compatible with the currently available models for the NS equation of state requires $2 \leq (R/R_s) \leq 4$. Here we take R in this range, with $M = 1.4M_\odot$. Let D be the distance from the star to the observer, and N_H the intervening column density. The flux measured by an observer at infinity is then given by the sum of the contributions from the thermal component and from the polar caps

$$F(E; \gamma) = \frac{\pi R^2 e^{-\Lambda_s}}{4\pi D^2} e^{-\sigma(E)N_H} \int_0^1 2x dx \int_0^{2\pi} \frac{d\phi}{2\pi} \times \left\{ \frac{1}{kT_p} \sigma T_{\text{th}}^4(\theta, \phi) n[EE^{-\Lambda_s}; T_{\text{th}}(\theta, \phi)] + \frac{1}{kT_{\text{hs}}} \sigma T_{\text{hs}}^4(\theta, \phi) n[EE^{-\Lambda_s}; T_{\text{hs}}(\theta, \phi)] \right\}, \quad (9)$$

in units of $\text{phot cm}^{-2} \text{ s}^{-1} \text{ keV}^{-1}$. Note that the dependence on γ comes in through Eqs. (1) – (3).

Finally, the energy dependent pulsed fraction is defined by

$$Pf(E) = \frac{F^{\text{max}}(E) - F^{\text{min}}(E)}{F^{\text{max}}(E) + F^{\text{min}}(E)}, \quad (10)$$

where $F^{\text{max}}(E)$ and $F^{\text{min}}(E)$ are, respectively, the maximum and minimum flux over a rotation period of the star. The phase of the pulsation, $Ph(E)$, is defined as the phase angle γ at which the flux is maximum at energy E .

3. Application to PSR 1055-52, PSR 0656+14 and PSR 0630+18

For each pulsar, we considered three types of models: a two-component blackbody (of the type expected from iron atmospheres), or a two-component light-element atmosphere, and for the latter we considered two different types of opacities. The emergent spectrum from iron atmospheres is similar to a blackbody in its gross properties (Rajagopal, Romani & Miller 1997) and we assume that it is moderately beamed as discussed in §2. The two-component light-element atmosphere is substantially bluer than a blackbody and also exhibits a hard tail. We have used two different semianalytic atmospheres of Heyl & Hernquist (1998c) with opacities decreasing as ν^{-3} and ν^{-1} . The former model is much bluer than a blackbody and exhibits a strong hard tail. The latter is most appropriate to model magnetized light-element atmospheres (*e.g.* Pavlov et al. 1994); it is intermediate between the ν^{-3} -model and the blackbody.

The effective temperatures (parameterized through T_p and T_{hs}) and the size of the hot region (called β in our paper) corresponding to the same effective blackbody temperatures are different in the three models, and, to precisely determine them in each case, we generated a simulated spectrum (using the software XSPEC, Arnaud 1996, and the *ROSAT* PSPC detector) of each object, using the temperature values of the double-blackbody fits and the ratio between the areas of the two components given in the literature. This spectrum was then fitted with the phase

averaged spectrum of our model⁴ to determine T_p , T_{hs} and β . These values were then used to compute pulsed fractions and phases with some choices of n_1 and n_2 .

We found that an iron-type atmosphere, which has a rather mild degree of beaming, was unable to reproduce the degree of modulation observed in the softest part of the spectrum (dominated by the thermal component⁵). A light element atmosphere with an opacity $\propto \nu^{-3}$ was able to reproduce reasonably well the pulsed fractions in the soft component of the spectrum. However, the tail of the thermal component is generally so strong that a second hotter component was not statistically required by the data in the case of PSR 0656 and PSR 1055, and it was much smaller than the one required by the double blackbody fit in the case of Geminga⁶. Such a model was unable to produce the sudden transition in the behaviour of the pulsed fractions accompanied by a phase shift around 0.5 keV which is observed in PSR 0656 and PSR 1055. Moreover, such models implied surface areas much larger than what would be consistent with any reasonable equation of state for the neutron star. A two-component atmosphere model which is less blue ($\propto \nu^{-1}$) than the former required a second hotter component in the spectral fitting, and was able to reproduce the behaviour of the observed pulsed fractions and phase shifts. More details on each of the object that we considered are given in the following.

3.1. PSR 1055-52

This pulsar has a characteristic age $\tau = P/2\dot{P} \sim 5 \times 10^5$ yr, and a rotational energy loss rate of $\dot{E} \sim 3 \times 10^{34}$ erg/sec. *ROSAT* observations (Ögelman & Finley 1993) clearly show that the pulses have an energy dependent phase and pulsed fraction, with a transition at ~ 0.5 keV. The pulsed fraction below the transition is roughly constant at a value on the order of 7-8%, while after the transition it rapidly increases to a maximum of 0.85 around 1 keV. The hard photons lead the soft ones by an angle $\sim 120^\circ$. A blackbody fit to the spectrum requires two components, with temperatures $T_{\text{soft}} \sim 8 \times 10^5$ K and $T_{\text{hard}} \sim 3.7 \times 10^5$ K, and a ratio between the areas of $A_{\text{soft}}/A_{\text{hard}} \sim 3 \times 10^{-5}$ (Greiveldinger et al. 1996). The angles ξ and χ have been inferred by Malov (1990) to be both about 30° . With these values, and T_p , T_{hs} and β calibrated on the phase averaged spectrum, we show the derived pulsed fractions and phase for this pulsar in Figure 1, having assumed $n_1 = 1$ and $n_2 = 2$.

⁴This is given by $\frac{1}{2\pi} \int_0^{2\pi} d\gamma F(E; \gamma)$.

⁵Note, however, that this result is dependent on the assumption of a dipolar field. The value of the pulsed fractions can be increased if a quadrupole component is added (Page & Sarmiento 1996).

⁶ Note that in the case of Geminga, similar results had been found by Meyer et al. (1990).

3.2. PSR 0656+14

PSR 0656+14 was discovered in an *Einstein* satellite survey of ultrasoft sources (Cordova et al. 1989). It has a relatively young spin down age of 1.1×10^5 yr and a rotational energy loss rate $\dot{E} \sim 3.8 \times 10^{34}$ erg/sec. The combined *ASCA* and *ROSAT* spectrum reveals two blackbody components with $T_{\text{soft}} \sim 8 \times 10^5$ K, and $T_{\text{hard}} \sim 1.5 \times 10^6$ K, and shows evidence that a power-law component is needed to account for higher energy photons. The ratio of the hot polar cap area to the neutron star surface area is $\sim 7 \times 10^{-3}$ (Greiveldinger et al. 1996).

As for PSR 1055-52, both the phase and the pulsed fraction are energy dependent. Below ~ 0.5 keV, the pulsed fraction stays a little under $\sim 10\%$, and it increases modestly in the range $0.5 - 1$ keV to around 20-30 % at 1 keV. The soft and the hard components are shifted in phase by about 85° with respect to each other. The angles ξ and χ have been estimated by Malov (1990) to be both about 35° . With these values, and T_p , T_{hs} and β derived from spectral fitting, we show the pulsed fraction and phase that our model predicts with the choice $n_1 = 0.8$ and $n_2 = 0.2$ in Figure 2.

3.3. PSR 0630+18 (Geminga)

Geminga was first observed as a high-energy γ -ray source with the SAS-2 satellite in the 100 MeV band (Fichtel et al. 1975). It was only in 1992 that it was observed in the X-ray band with *ROSAT* (Halpern & Holt 1992). Its period and spin-down rate (Bertsch et al. 1992; Hermsen et al. 1992) yield a dynamic age of 3.4×10^5 yr, and a rotational energy loss rate $\dot{E} \sim 3.5 \times 10^{35}$ erg/sec. A spectral analysis of the *ROSAT* data made by Halpern & Ruderman (1993) shows that the X-ray spectrum consists of two blackbody components with $T_{\text{soft}} \sim 5 \times 10^5$ K, and $T_{\text{hard}} \sim 3 \times 10^6$ K. Both components are modulated at the pulsar rotation period, but the harder X-ray pulse leads the soft pulse by about 105° in phase. Geminga is believed to be an orthogonal rotator, with $\xi = \chi \sim 90^\circ$ (Malov 1990).

Unlike PSR 1055-52 and PSR 0656+14, the pulsed fraction observed in Geminga shows a decrease with energy at low energies: the amplitude of the pulsations in the PSPC channels 8-28 (i.e. roughly at energies below 0.3 keV) is much larger than in channels 28-53 (roughly corresponding to the energy range 0.3-0.5 keV): 33% versus 20%. Figure 3 shows that a significant decrease of the pulsed fractions in the 0.3-0.5 keV energy range can be reproduced with the model described in §2: here we have taken $n_1 = 1.5$ and $n_2 = 3$, while all other model parameters have again been calibrated from a fit to the phase-averaged spectrum⁷. The decrease in the pulsed fraction occurs in the region where the harder component starts to overtake the softer one. The hard component brings more photons at phase angles in which the soft component has less

⁷Note that a similar behaviour for the *Pfs* in the softest part of the spectrum could be obtained with a more modest beaming (i.e. smaller n_1), but a quadrupole component of the *B* field added to the dipole (Page96).

photons, therefore leading to a decrease of the intensity fluctuations produced by the thermal component alone. This effect happens in the same way also in the other two examples that we showed, but due to the less intense beaming of the harder component assumed there, the decrease is not so pronounced. Interestingly, a slight decrease in the pulsed fraction before its rapid increase can be observed also in the data for these other two pulsars (e.g. Ögelman 1995).

Our model for the phase shifts and pulsed fraction in Geminga is similar to that proposed by Halpern & Ruderman (1993). Page, Shibano & Zavlin (1995) later argued that this picture could not work because the flux in the hard component is more than an order of magnitude less than that in the soft component in the 0.3 – 0.5 keV energy range, where the decrease in the Pf is observed. However, the pencil-beaming reduces the flux of the soft component at the same phase of the rotation where the fan-beaming of the hard component increases its flux; therefore, although the phase averaged fluxes in the two components are not comparable, the instantaneous fluxes at $\gamma \sim 90^\circ$ can be, and the hard component can begin to influence the soft one well before it becomes dominant in the phase-averaged spectrum.

4. Summary and Discussion

We have proposed a simple model that is able to account for properties of the X-ray emission observed in the three middle aged pulsars PSR 1055-52, PSR 0656+14 and Geminga within a unified framework. The emission in the $\sim 0.1 - 1$ keV energy range is believed to be due to the combination of thermal radiation from the entire star and emission from heated polar caps. We have argued that, while pencil beaming is expected for the thermal, soft component, the hard component from the polar caps is expected to be beamed into a fan, as discussed in the literature for similar problems in other contexts. We have shown that such a model is able to account not only for the magnitude of the pulsations in PSR 1055-52 and PSR 0656+14, but also for the phase shifts between the soft and the hard component observed in all the three objects. We have shown that this same model is able to reproduce also the decrease of the pulsed fraction observed in the soft X-ray emission of Geminga, without requiring any special model for the composition of the surface of this object. However, we have found that the type and composition of the atmosphere plays an important role. An atmosphere made of heavy elements is not able to account for significant Pfs (if only a dipolar field is assumed for the thermal component), while a light element atmosphere with opacity $\propto \nu^{-3}$ has a very pronounced tail which is able to account for the all spectrum (up to about 1.5 - 2 keV) for PSR 0656 and PSR 1055, without requiring a second, hotter component. Such a model is not able to account for the sudden increase of the Pfs (accompanied by a phase shift) that is observed for these two pulsars around 0.5 keV. In the case of Geminga, the implied size of the hot spots is too small to produce any significant effect. On the other hand, a light element atmosphere with opacity $\propto \nu^{-1}$ requires a second, hotter component to account for the overall spectrum, and, as we have shown, such a model is able to account for the observed pulsed fractions and phase shifts, if one allows the emission from the hot spots to have a

variable degree of beaming for the various objects. We have argued that this is plausible, as it depends on the spatial and energy distribution of the bombarding particles, which is likely to vary among the various objects.

In conclusion, we need to stress that the model we have presented here was aimed at explaining features observed in the X-ray emission from middle aged pulsars from a qualitative point of view. A more quantitative analysis, which includes detector and absorption effects⁸ would not change any of the qualitative features reproduced here. On the other hand, a thorough analysis, inclusive of detailed predictions for the shape of the pulse profiles, would require very detailed models for the atmosphere and for the temperature distribution on the star, as well as much better data with which to compare the model. We anticipate that forthcoming observational data from the *Chandra* and *XMM* missions will soon make this endeavor feasible.

We thank Jonathan McDowell for support with use of the XSPEC software.

REFERENCES

- Arnaud, K. A. 1996, in ASP Conf. Series 101, *Astronomical Data Analysis Software and Systems V*, ed. G. Jacoby & J. Barnes (San Francisco: ASP), 17
- Bertsch, D. L. *et al.* 1992, *Nature*, **357**, 306.
- Becker, W. & Trumper, J. 1997, *A&A*, **326**, 682
- Chiu, H.-Y. & Salpeter, E. E. 1964, *Phys. Rev. Lett.*, **12**, 413.
- Cordova, F. A., Middleditch, J., Hjellming, R. M. & Mason, K. O. 1989, *ApJ*, **345**, 451.
- Fichtel, C. E. *et al.* 1975, *ApJ*, **198**, 163.
- Greenstein, G. & Hartke, G. J. 1983, *ApJ*, **271**, 283.
- Greiveldinger, C. *et al.* 1996, *ApJL*, **465**, 35.
- Halpern, J. P. & Holt, S. S. 1992, *Nature*, **357**, 222.
- Halpern, J. P. & Ruderman, M. 1993, *ApJ*, **415**, 286.
- Hermesen, W. *et al.* 1992, IAU Circular No. 5541
- Heyl, J. S. & Hernquist, L. 1998a, *MNRAS*, **300**, 599.

⁸For a perfect (diagonal) detector, absorption does not affect the *energy-dependent Pfs* (but it does affect the *Pf* over a finite energy bandwidth; Perna *et al.* 2000); however, for a real detector, absorption can affect also the energy-dependent *Pfs* to a certain extent (Page 1995).

- Heyl, J. S. & Hernquist, L. 1998b, *MNRAS*, **297**, L69.
- Heyl, J. S. & Hernquist, L. 1998c, *MNRAS*, **298**, L17.
- Heyl, J. S. & Hernquist, L. 2000, *MNRAS*, in press
- Malov, I. F. 1990, *Astron. Zh.*, **67**, 377., *Sov. Astron.*, 34, 189
- Meyer, R. D., Pavlov, G. G., & Meszaros, P. 1994, *ApJ* **433**, 265
- Milgrom, M. & Salpeter, E. E. 1975, *ApJ*, **196**, 583.
- Ögelman, H. 1995, in M. A. Alpar, U. Kiziloglu & J. V. Paradijs (eds.), *The Lives of Neutron Stars*, p. 101, Kluwer, Dordrecht
- Ögelman, H. & Finley, J. P. 1993, *ApJL*, **413**, 31.
- Page, D. 1995, *ApJ*, **442**, 273.
- Page, D. & Sarmiento, A. 1996, *ApJ*, **473**, 1067.
- Page, D., Shibanov, Y. A. & Zavlin, V. E. 1995, *ApJL*, **451**, 21.
- Pavlov, G. G., Shibanov, Y. A., Ventura, J. & Zavlin, V. E. 1994, *A&A*, **289**, 837.
- Perna, R., Heyl, J., & Hernquist, L. 2000, *ApJL*, **538**, 159.
- Rajagopal, M., Romani, R. W., & Miller, M. C. 1997, *ApJ*, **479**, 347.
- Shibanov, Y. A., Pavlov, G. G., Zavlin, V. E. & Tsuruta, S. 1995, in H. Böhringer, G. E. Morfill & J. E. Trümper (eds.), *Seventeenth Texas Symposium on Relativistic Astrophysics and Cosmology*, Vol. 759 of *Annals of the New York Academy of Sciences*, p. 291, The New York Academy of Sciences, New York
- Tsuruta, S. 1964, *Ph.D. thesis*, Columbia University
- Zane, S., Turolla, R. & Treves, A. 2000, *ApJ*, **537**, 387.
- Zavlin, V. E., Pavlov, G. G. & Shibanov, Y. A. 1996, *A&A*, **315**, 141.

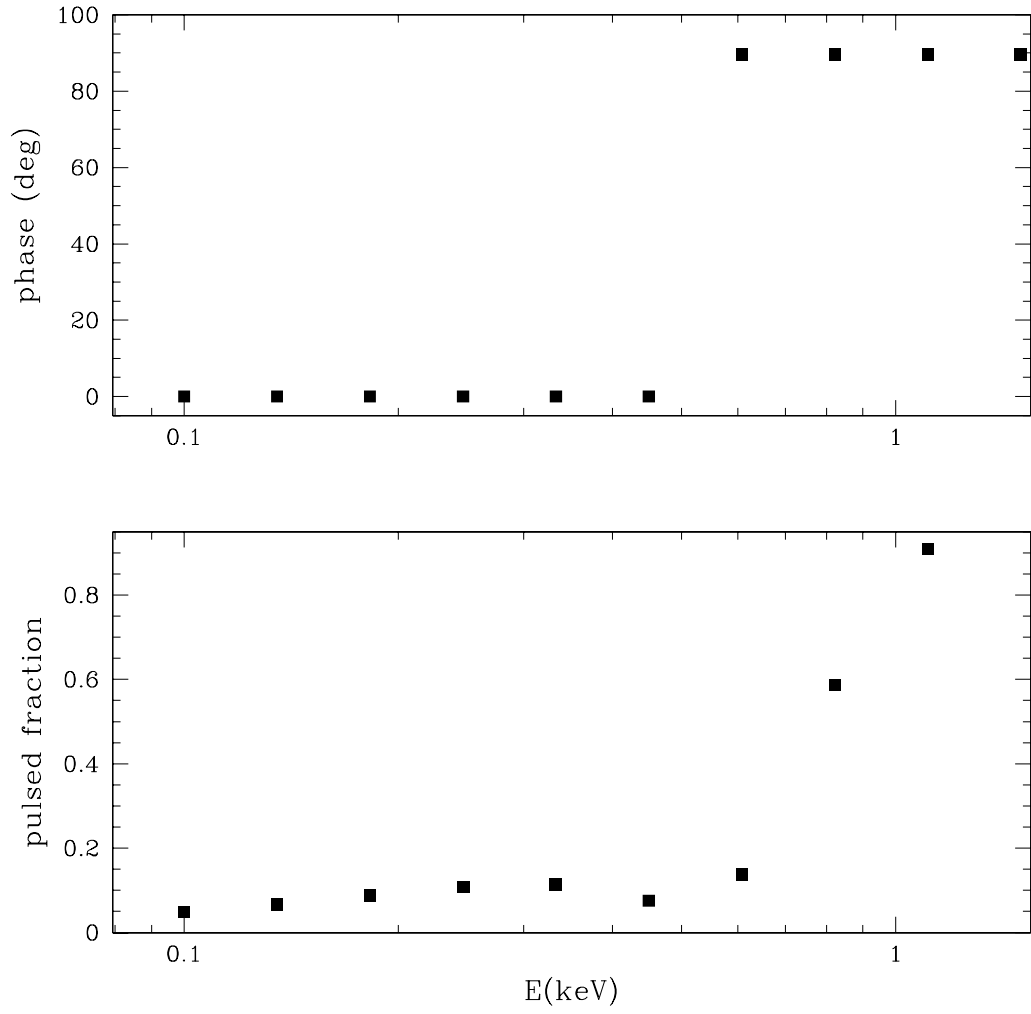


Fig. 1.— Predicted energy-dependent phase and pulsed fraction for the X-ray emission from PSR 1055-52.

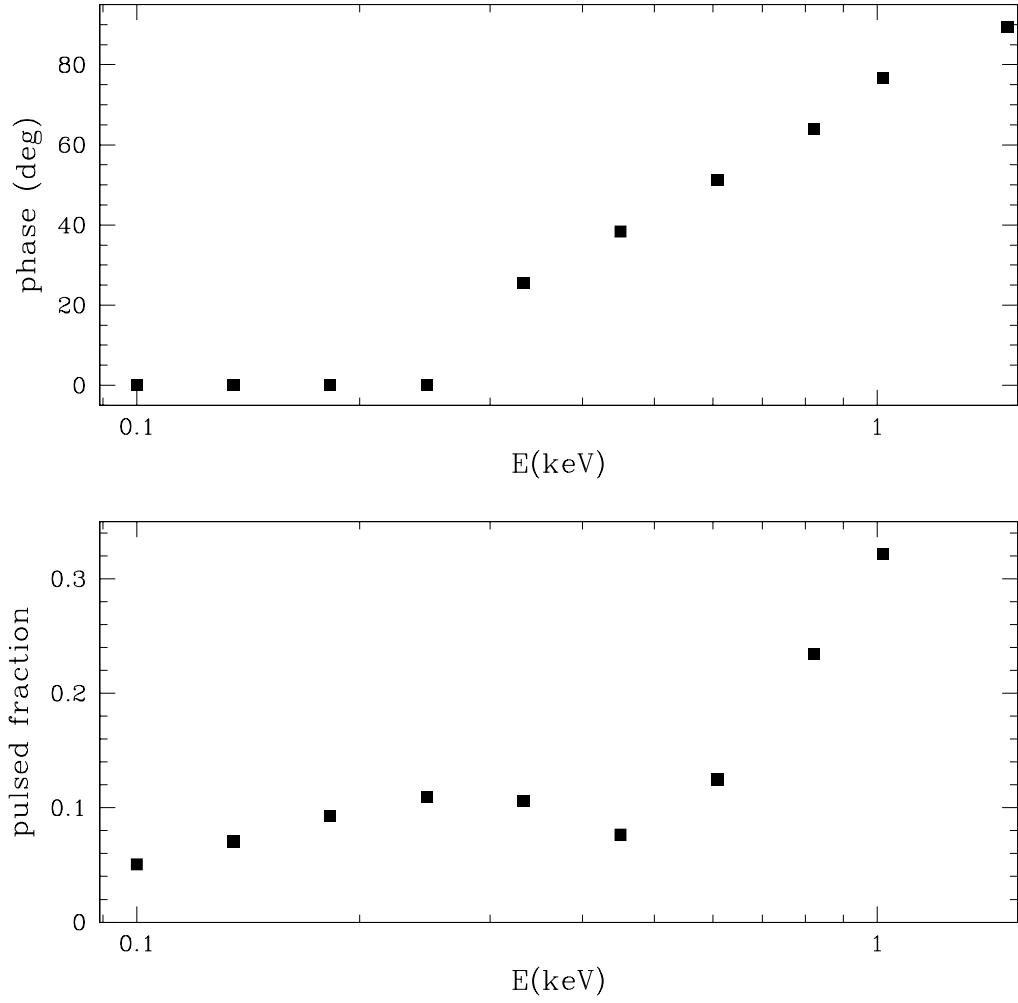


Fig. 2.— Predicted energy-dependent phase and pulsed fraction for the X-ray emission from PSR 0656+14.

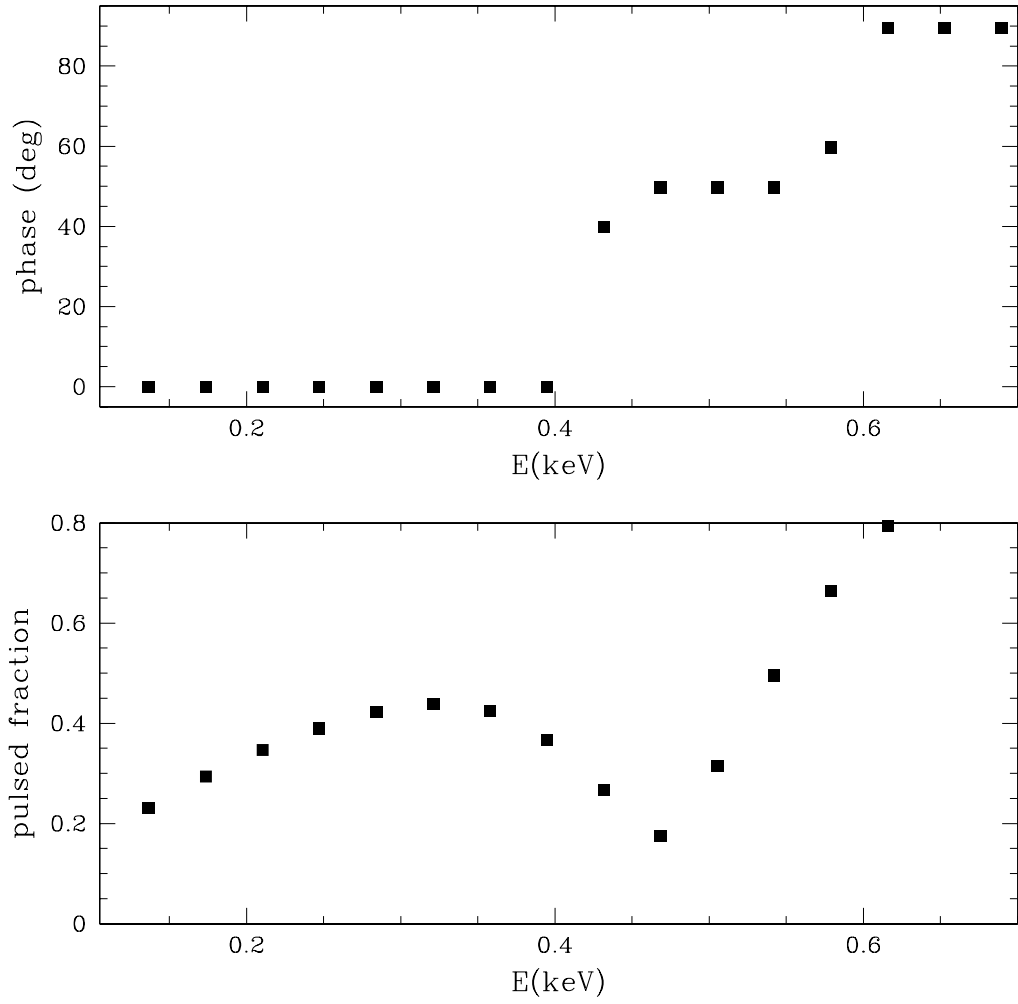


Fig. 3.— Predicted energy-dependent phase and pulsed fraction for the X-ray emission from Geminga.